THE JOURNAL OF PHYSICAL CHEMISTRY LETTERS
A JOURNAL OF THE AMERICAN CHEMICAL SOCIETY

pubs.acs.org/JPCL Letter

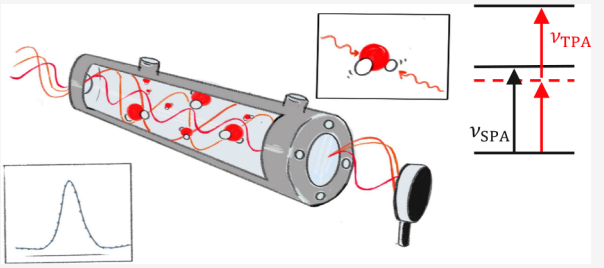
# Direct Precision Measurement of the $4\nu_3$ Band Origin in $H_2{}^{16}O$ by Intracavity Two-Photon Absorption

Arthémise Altman, Frank M. J. Cozijn, Alexandr S. Bogomolov, Roland Tóbiás, Attila G. Császár, Wim Ubachs, and Clément Lauzin*

Cite This: https://doi.org/10.1021/acs.jpclett.6c02007 Read Online

ACCESS | Metrics & More | Article Recommendations | Supporting Information

**ABSTRACT:** A novel spectroscopic approach combining wavelength-modulated Noise-Immune Cavity-Enhanced Optical-Heterodyne Molecular Spectroscopy (wm-NICE-OHMS) and two-photon absorption (TPA) is employed to directly determine the energy of the $4\nu_3$ vibrational band origin in $H_2{}^{16}O$ from a single spectroscopic transition. The resulting excitation energy, $E/h$ = 435 823 319 572.0 ± 4.6 kHz, is 4 orders of magnitude more accurate than previous determinations based on conventional spectroscopy (35 MHz uncertainty). This measurement provides a stringent benchmark for first-principles calculations in the third stretching overtone region of water. In addition, TPA enables direct connections between opposite-parity states within a vibrational manifold, thereby strengthening a recently established, high-accuracy spectroscopic network of $H_2{}^{16}O$.




Cavity-enhanced molecular absorption spectroscopy has emerged as a powerful and widely explored tool for applications,[1] ranging from ultrahigh accuracy frequency metrology,[2,3] setting an SI-temperature standard,[4,5] to tests of fundamental physics.[6,7] Among the available techniques, the variant of wavelength-modulated Noise-Immune Cavity-Enhanced Optical-Heterodyne Molecular Spectroscopy (wm-NICE-OHMS) has demonstrated exceptional sensitivity for the detection of single-photon absorption (SPA) transitions.[8,9] More recently, the possibility of two-photon absorption (TPA) in the rovibrational quantum level structure of molecules was added to the toolkit of continuous-wave cavity-enhanced spectroscopy.[10,11]

The TPA technique was suggested[12] and demonstrated[13] in the early days of atomic laser spectroscopy. The use of counter-propagating laser beams makes it a Doppler-free technique with the additional advantage that the photon recoil shift is canceled. The single-beam contribution to two-photon absorption[14] leads to a weak and broad background which will be neglected in the present study. In contrast to saturation spectroscopy, all molecules, regardless of their velocities, participate in the TPA signal. In the application of TPA to rovibrational molecular transitions, a necessity was identified of a real intermediate state with small detuning from the virtual intermediate level of the TPA resonance. In the original proposal,[10] only a single TPA line in an entire vibrational band of $CO_2$ was suggested to exhibit sufficient enhancement. In a subsequent demonstration experiment in $N_2O$,[11] only a signal on a specific Q(18) two-photon line in an overtone band, enhanced by a R(17) single-photon line at detuning 3.4 GHz (0.113 $cm^{-1}$), was detected. The combination of the TPA technique with cavity-enhanced spectroscopy was recently employed for trace gas detection[15] and the detection of $^{14}CO_2$.[16]

In the present study, it is demonstrated that TPA allows the direct determination of the $4\nu_3$ vibrational band origin of the $H_2{}^{16}O$ molecule at high absolute accuracy. Water is an asymmetric rotor molecule and with its dense quantum level structure it provides a favorable situation where many intermediate levels are available for providing the required enhancement for TPA. The quantum-level scheme of the water molecule for probing the two-photon transition from the $(000)0_{0,0}$ ground state of para-$H_2{}^{16}O$ to the $(004)0_{0,0}$ excited state for a direct measurement of the $4\nu_3$ band origin is shown in Figure 1. While the single-photon transition is forbidden due to symmetry reasons ($J' = 0 \nleftarrow J'' = 0$), the TPA transition is enhanced by an intermediate level $(101)1_{0,1}$ detuned from the virtual intermediate state by some 127 GHz, well outside the Doppler width of the single-photon transition $(101)1_{0,1} \leftarrow (000)0_{0,0}$. From the carefully established line list of TPA resonances, no alternative assignments were found as possible TPA lines at the detected frequency. Inspection of the level structure of $H_2{}^{16}O$ revealed that other intermediate levels, $(200)1_{1,1}$, $(002)1_{1,1}$ and $(021)1_{0,1}$ enhance the same TPA, but

Received: June 18, 2026
Revised: July 27, 2026
Accepted: August 11, 2026

ACS Publications © XXXX American Chemical Society



Downloaded from pubs.acs.org/jpclcd/article-pdf/doi/10.1021/acs.jpclett.6c02007/6742872/acs.jpclett.6c02007.pdf by UNIV CATHOLIQUE DE LOUVAIN user on 27 August 2026

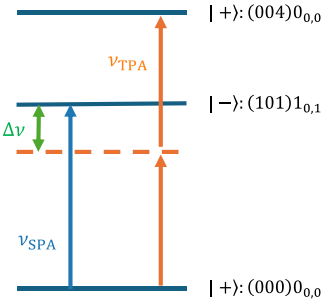



**Figure 1.** Representation of the TPA scheme used in $H_2O$. SPA at $\nu_{SPA}$, and TPA at frequency $\nu_{TPA}$ by passing through a virtual intermediate state, detuned by $\Delta\nu$ from a real resonance (in this case 127 GHz). Parity assignments are given as $|\pm\rangle$ and vibrational and rotational quantum numbers as $(\nu_1\ \nu_2\ \nu_3)\ J_{K_a,K_c}$.

in view of their much larger detunings (958 GHz, 6632 GHz, and 11200 GHz, respectively) and of the quadratic dependence, the effect is minute.

Compared to state-of-the-art cavity-enhanced TPA studies in linear molecules,[11,15,16] the present study introduces three key technical advances. First, we apply the wm-NICE-OHMS technique that provides the extreme sensitivity necessary to probe two-photon transitions at very low pressures (≈ 0.1 Pa). This spectrometer was specifically designed to measure weak saturated absorption Lamb dips in quadrupole transitions at high intracavity power,[17] a regime highly similar to measuring TPA resonances. Accessing this low-pressure regime allows us to operate in the collision-free transit-time limit. Second, we show for the first time that Doppler-free TPA lines can be significantly narrower than corresponding SPA lines, a phenomenon previously obscured by pressure broadening. Third, we demonstrate that the dense rovibrational manifold of an asymmetric top molecule like water facilitates strong TPA signals despite the massive intermediate state detuning noted above (127 GHz, compared to 3 to 5 GHz in previous studies[11,15]). This establishes TPA as a broadly applicable precision tool for asymmetric molecules rather than a technique limited to cases with fortuitous resonances.

Leveraging these technical advances, the targeted $(004)0_{0,0} \leftarrow (000)0_{0,0}$ two-photon transition was measured with few-kHz accuracy (see the Experimental Method section). Data from a typical recording is shown in Figure 2. An important signature for assigning the resonance as TPA lies in the fact that the signal is reversed in sign with respect to the many Lamb dip features observed. Although the pure transit-time limit for a two-photon resonance predicts a sharp cusp,[18] physical mechanisms such as residual pressure broadening and the applied wavelength modulation dither round off this feature into a profile that is excellently approximated by a standard Lorentzian (see the Supporting Information). Consequently, the demodulated signal can be modeled using the 1*f*-derivative of a dispersive Lorentzian. While this functional form is conventionally employed for single-photon saturated-absorption (Lamb-dip) measurements,[19−21] we find that it empirically reproduces the observed TPA resonances just as well. We therefore determine the center resonance frequency by fitting the data to the following expression:

$$S(\nu) = A\frac{\Gamma^2 - 4(\nu - \nu_{fit})^2}{(\Gamma^2 + 4(\nu - \nu_{fit})^2)^2} + B \quad (1)$$

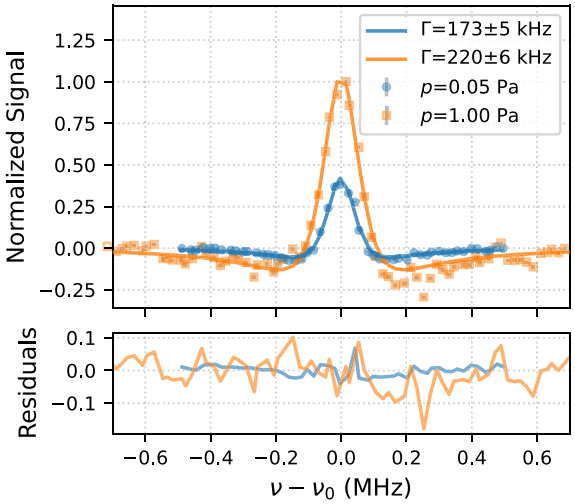



**Figure 2.** Recordings of the $(004)0_{0,0} \leftarrow (000)0_{0,0}$ TPA resonance with wm-NICE-OHMS. These two single-scan spectra were obtained in 8 min, the first at a pressure setting of 0.05 Pa, 183 W of intracavity circulating power and 130 kHz dither amplitude (blue dots), while the second one at 1.00 Pa, 69 W of intracavity circulating power, and 65 kHz dither amplitude (orange squares). The blue and orange lines represent fitted TPA line profiles following eq 1, with residuals displayed in the bottom panel.

where $S(\nu)$ is the demodulated signal as a function of frequency $\nu$. The fit parameters are the line center $\nu_{fit}$, the amplitude $A$, the FWHM line width parameter $\Gamma$, and a constant vertical offset $B$. The presently obtained width, around 175 kHz at 0.05 Pa, is significantly narrower than that of SPA Lamb dips of water measured at the same wavelength and under identical pressure conditions (≈ 300 kHz).[21] The dominant causes of this residual line broadening are expected to be transit-time and pressure broadening, with a minor contribution from power broadening.

For each pressure and power setting a series of measurements, typically comprising 16 scans, was performed to determine the line-center frequencies. The frequencies determined from the individual scans were subsequently averaged and the standard error of the mean was evaluated. An example is presented in Figure 3. For the spread of data points see the Methods section.

The two-photon resonance frequency is affected by the intracavity pressure and the circulating power level. Thus, the line position has to be corrected for these systematic effects. The unperturbed transition frequency is extracted by applying a 2D linear regression to the comprehensive data set consisting of frequencies determined in a range of pressure and power levels, whereby each data point is obtained as an average over multiple scans. We model the measured transition frequency $\nu(P, W)$ as follows:

$$\nu(P, W) = \nu_{0,0} + c_p P + c_w W \quad (2)$$

where $c_p$ is the linear pressure shift coefficient (in kHz/Pa) and $c_w$ is the linear power shift coefficient (in kHz/W). The data set comprises more than 55 experimental points acquired on different days, each typically representing the average of 16 scans. A weighted fit, using the combined statistical and clock uncertainty of each point, yields the pressure- and power-shift coefficients and the intercept, $\nu_{0,0}$. The latter represents the

Downloaded from pubs.acs.org/jpclcd/article-pdf/doi/10.1021/acs.jpclett.6c02007/6742887/2/acs.jpclett.6c02007.pdf by UNIV CATHOLIQUE DE LOUVAIN user on 27 August 2026


https://doi.org/10.1021/acs.jpclett.6c02007
J. Phys. Chem. Lett. XXXX, XXX, XXX−XXX

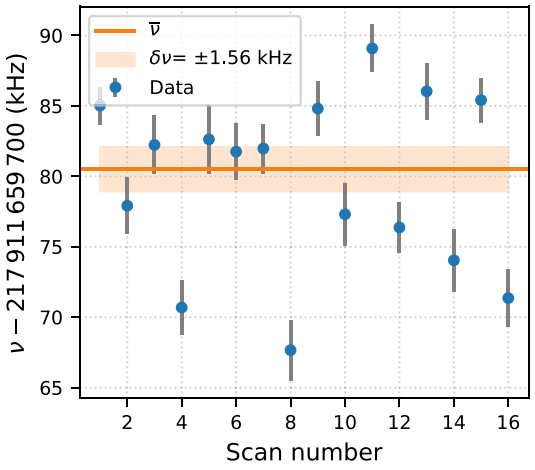



**Figure 3.** Weighted average (orange line) of line centers of the $(004)0_{0,0} \leftarrow (000)0_{0,0}$ two-photon resonance obtained from a series of scans at 1.00 Pa and 69 W of intracavity power (blue dots) and standard error of the mean (orange filled area). Resulting value for these conditions is $\nu$ = 217 911 659 780.51 (1.56) kHz. All stated uncertainties and error bands represent 1$\sigma$ intervals.

extrapolated frequency at the zero-pressure, zero-power limit. The results of this fit are presented in Table 1.

**Table 1. Results of the 2D Linear Regression Analysis Modeling the Pressure and Power Dependencies of the $(004)0_{0,0} \leftarrow (000)0_{0,0}$ Two-Photon Transition Frequency[a]**

| Parameter | Fit result | Uncertainty |
|---|---|---|
| $\nu_{0,0}$ (kHz) | 217 911 659 785.7 | 2.1 |
| $c_p$ (kHz/Pa) | −2.8 | 1.2 |
| $c_w$ (kHz/W) | −0.02 | 0.03 |

[a]The extrapolated zero-pressure, zero-power line center is given by $\nu_{0,0}$, while $c_p$ and $c_w$ represent the pressure and power shift coefficients, respectively. All stated uncertainties represent 1$\sigma$ intervals.

Figure 4 shows a slice of the 2D fit and our frequency measurements as a function of pressure at 69 W. The frequency at 0 Pa is nonzero because of the power shift.

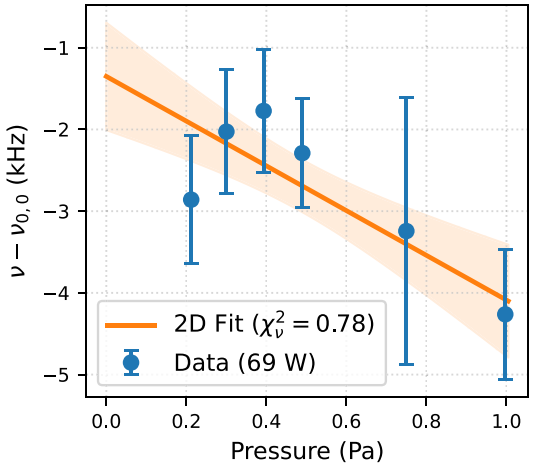



**Figure 4.** Slice of the 2D fit showing the pressure shift of the $(004)0_{0,0} \leftarrow (000)0_{0,0}$ two-photon resonance measurements at 69 W of circulating laser power. The individual measurements for each pressure are averaged for legibility.

This shift, primarily originating from the AC Stark effect, is shown to be only a minor cause for line shifts. Given our circulating power of 69 W, the coefficient $c_w$ = − 0.02 ± 0.03 kHz/W translates to a frequency offset of only ≈1.4 kHz, which is corrected for in the extrapolated $\nu_{0,0}$ frequency. Furthermore, the absence of structure in the residuals observed in the individual line fits (as shown in Figure 2) confirms that the near-resonant TPA process does not suffer from significant line shape distortion caused by intracavity intensity inhomogeneity. The pressure shift coefficient obtained lies in the same range, [-20,+20] kHz/Pa, as found for the measurements of Lamb dips in both $H_2{}^{16}O$[19,20] and $H_2{}^{18}O$.[22] It was verified in previous studies that wavelength-modulation effects do not cause line shifts even at a 100-Hz accuracy level.[21,23]

As for broadening of the TPA line profile, there are also two dominant contributions, related to pressure and transit time, while power broadening is a smaller effect. Figure 5 illustrates

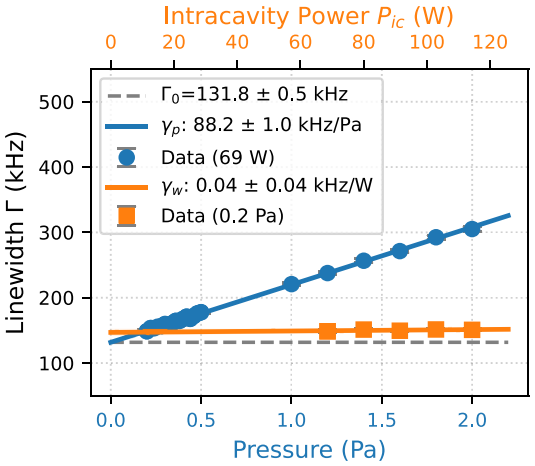



**Figure 5.** Fitted pressure broadening ($\gamma_p$, blue line) and power broadening ($\gamma_w$, orange line) of the $(004)0_{0,0} \leftarrow (000)0_{0,0}$ two-photon resonance for measurements made at 69 W of intracavity power (blue dots) and 0.2 Pa (orange squares) respectively.

the full-width at half-maximum (FWHM) line width Γ of the two-photon resonance as a function of pressure, recorded at a constant intracavity power, and as a function of intracavity power, recorded at a constant pressure. Extrapolating these measurements to zero pressure yields an intrinsic line width of $\Gamma_0$ = 131.6 ± 1.1 kHz. This TPA width is strikingly narrower than typical SPA widths (≈ 290 kHz) obtained for water under similar Doppler-free conditions.[19−21]

This difference between the TPA and SPA (Lamb-dip) widths reflects the fundamentally different physical mechanism of the two-photon process. For a Gaussian beam with a waist radius of $w_0$ = 0.71 mm, the standard SPA average transit-time broadening for a gas at thermodynamic equilibrium ($T$ = 300 K) is $\Delta\nu_{SPA} = u/(\pi\, w_0)$,[24] where $u = \sqrt{2k_BT/m} \approx 526$ m/s is the most probable radial speed. This yields a theoretical limit of ≈ 236 kHz. Previously measured SPA Lamb dips (∼ 290 kHz) align with this baseline when accounting for residual pressure, power broadening, and wavelength modulation dither broadening.

In contrast, Doppler-free TPA is a second-order process where the weak-field transition probability scales as $1/v_r^2$ where $v_r$ is the radial velocity. This scaling induces a selection of slow-moving molecules, spending longer times in the laser field. The

Downloaded from pubs.acs.org/jpclcd/article-pdf/doi/10.1021/acs.jpclett.6c02007/6742887/2/acs.jpclett.6c02007.pdf by UNIV CATHOLIQUE DE LOUVAIN user on 27 August 2026


https://doi.org/10.1021/acs.jpclett.6c02007
J. Phys. Chem. Lett. XXXX, XXX, XXX−XXX

thermally averaged, transit-time limited FWHM for this TPA process was originally formulated by Lehmann.[18] The theoretical limit is given by $\Delta\nu_{TPA} = \ln(2)u/(2\pi w_0)$, predicting a theoretical limit of ≈ 82 kHz for our setup. Our extrapolated intrinsic line width of $\Gamma_0$ = 132 kHz falls somewhat above that limit, largely due to broadening caused by the dithering applied to enhance SNR.

To account for small systematic frequency shifts, we consider the full relation between the measured photon energy and the zero-pressure zero-power quantum level separation of frequency $\nu_0$. For a single-photon line, this is given by[25]

$$h\nu_{0,0} = h\nu_0 \pm \frac{h\vec{k}\cdot\vec{v}}{2\pi} - \frac{(h\nu_0)v^2}{2c^2} \pm \frac{(h\nu_0)^2}{2mc^2} \quad (3)$$

The term with $\vec{k}\cdot\vec{v}$ represents the first-order Doppler effect, while the last two terms represent the second-order Doppler shift and the photon recoil effect, respectively.

The primary advantage of intracavity TPA spectroscopy is that the absorption of two counter-propagating photons results in the cancellation of the first-order Doppler effect and in zero net momentum transfer to the molecule, which cancels the photon recoil shift. Therefore, only the second-order Doppler shift (SODS):

$$\Delta\nu_{SODS} = -\nu_0\frac{\langle v^2\rangle_{eff}}{2c^2} \quad (4)$$

requires consideration, where $\nu_0$ is the zero-pressure zero-power laser frequency and $\langle v^2\rangle_{eff}$ is the mean-squared velocity of the molecular population contributing to the signal. In a gas at thermodynamic equilibrium at 300 K, the 3D most probable speed would yield a full thermal SODS of 0.5 kHz. However, without going into a detailed quantitative analysis, the molecules spending the longest time in the laser beam would contribute the most to the two-photon signal. We therefore crudely estimate a SODS correction of 0.3 ± 0.2 kHz, therewith covering the possibility whether or not intrinsic selection of slow molecules occurs by the TPA process.

The final corrected frequency presented in Table 2 represents the unperturbed experimental laser frequency for the TPA-transition $(004)0_{0,0} \leftarrow (000)0_{0,0}$, extrapolated to zero pressure and power, and corrected for the second-order Doppler shift. As the transition is excited from the ground state of *para*-$H_2{}^{16}O$, $(000)0_{0,0}$, this provides a direct measurement of the $4\nu_3$ band origin at exactly twice the measured corrected laser frequency:

$$\nu_{4\nu_3} = 435823319572.0 \pm 4.6\ \text{kHz} \quad (5)$$

**Table 2. Final Results of the Weighted Least Squares Regression Analysis**[a]

| | Result | Uncertainty |
|---|---|---|
| $\nu_{0,0}$ | 217 911 659 785.7 | 2.1 |
| SODS Correction | +0.3 | 0.2 |
| Final Frequency | 217 911 659 786.0 | 2.3 |

[a]The final, corrected laser frequency $\nu_0$ includes the second-order Doppler shift correction. All values are in units of kHz. Uncertainties correspond to a 1$\sigma$ interval.

## SPECTROSCOPIC NETWORK

The conventional way of representing energy levels in a molecule starts from an effective Hamiltonian (EH) leading to a functional form involving quantum numbers and molecular constants related to electronic, vibrational and rotational motions in the molecule. A commonly used expression for representing the rovibrational energy levels of a diatomic molecule is the Dunham expansion:[26]

$$E(v, J) = \sum_{k,l} Y_{k,l}\left(v + \frac{1}{2}\right)^k [J(J+1)]^l \quad (6)$$

where $v$ and $J$ are the vibrational and rotational quantum numbers and $Y_{k,l}$ are the Dunham coefficients. The vibrational band origins, which do not correspond to directly measurable SPA transitions, and other molecular constants are subsequently obtained through least-squares fitting to transitions measured between the manifolds of ground and excited states. To reproduce highly accurate experimental data in these fits, a large number of constants related to centrifugal distortion and anharmonic vibrations are often required. For polyatomic molecules, the situation becomes more complex in view of the centrifugal cross terms that have to be invoked. For the water molecule, there exists the interesting example of this approach, whereby a manifold of 749 energy levels in the first hexad of water levels (involving six interacting vibrations)[27] were included in a least-squares fit. The resulting 96-parameter model agrees with experiment only at the GHz level.[28]

The spectroscopic accuracy for water lines, based on cavity-enhanced techniques allowing for Lamb-dip measurements calibrated by frequency combs, has progressed to the kHz level of accuracy, 6 orders of magnitude better than the fitting accuracy achieved in ref 28. For this reason, spectroscopic networks,[29] which are able to retain the prediction accuracy at the experimental level, offer a better representation of the measured transitions.[19,20] The network also delivers level energies at the accuracy of present-day metrology experiments, where the effective Hamiltonian approach is orders of magnitude away. A drawback of the network approach is that it does not reveal the presence of local perturbations in the rotational progressions of the levels.

The power of such networks further lies in the fact that they help to design and optimize experimental measurement campaigns. For example, based on a limited set of precision measurements[30] it allowed the determination of a significant number of radio-line frequencies at a precision not achieved by direct microwave spectroscopy.[21,31] A missing ingredient for establishing the network is the connection between equal parity states in the rovibrational transitions measured in laser-based studies. In the most recent version of the ultraprecise $H_2{}^{16}O$ and $H_2{}^{18}O$ networks, reaching an accuracy at the level of 1−10 kHz,[19−21,30,31] the connection between quantum levels of (+) and (−) parity in the (0 0 0) ground vibrational manifold was established at a few-kHz accuracy via microwave transitions.[32−34]

A novelty that TPA resonances bring for spectroscopic networks is that connections between rotationless states can be established in a direct manner. In fact, many parity-conserving transitions in the rovibrational structure, not accessible via SPA, can be probed via TPA. Moreover, these connections can be made with high accuracy, due to the intrinsic Doppler-free nature of TPA if counter-propagating beams are used. The combination of SPA and TPA Doppler-free transitions in a

Downloaded from pubs.acs.org/jpclcd/article-pdf/doi/10.1021/acs.jpclett.6c02007/6742887/2/acs.jpclett.6c02007.pdf by UNIV CATHOLIQUE DE LOUVAIN user on 27 August 2026



https://doi.org/10.1021/acs.jpclett.6c02007
J. Phys. Chem. Lett. XXXX, XXX, XXX−XXX

network will provide a preferred method for producing a high-accuracy, well-connected spectroscopic network.

The $(004)0_{0,0}$ state was included previously in a prevailing spectroscopic network for the $H_2{}^{16}O$ molecule.[35] Its frequency was stated at 435 823 411 ± 35 MHz. The difference between our measurement and this value is 91 MHz, within $3\sigma$ of the previous experimental value, which was extracted from measurements made with a Fourier-transform spectrometer on the transition $(004)0_{0,0} \leftarrow (000)1_{1,1}$ with uncertainties ranging from 35 to 90 MHz.[36,37] This provides evidence for an unambiguous assignment of the TPA transition reaching the $4\nu_3$ vibrational band origin.

This single-line measurement offers unique leverage over traditional multiline measurements. While broadband spectroscopy is excellent for the statistical mapping of a rovibrational band, determining the band origin typically requires extrapolating back to the $J = 0$ state using complex effective Hamiltonians. For highly excited states in water, these empirical models suffer from severe parameter correlation and convergence issues due to centrifugal distortion and Coriolis resonances. By directly measuring the $(004)0_{0,0} \leftarrow (000)0_{0,0}$ transition, our TPA approach entirely bypasses these rotational complexities. It isolates the pure vibrational energy gap, providing a completely model-independent benchmark of the molecular potential energy surface. Furthermore, global theoretical line lists used in astrophysics and atmospheric sciences frequently rely on empirical shifts to correct their calculated vibrational band origins. Providing a highly accurate anchor for the $4\nu_3$ origin rigidly constrains these theoretical models and significantly improves the predictive accuracy of the entire corresponding vibrational band.

Based on Doppler-free TPA transitions, spectroscopic networks at kHz accuracy can now be extended to the higher excitation region of the water molecule, thereby gaining orders of magnitude in accuracy. The presently obtained highly accurate excitation energy of 14 500 $cm^{-1}$ represents a benchmark for the construction of first-principles water line lists. This transition frequency determination is of special interest since it reaches a state located above the barrier to linearity, where calculations become even more challenging.[38]

In summary, we report on the first direct measurement of the $4\nu_3$ vibrational band origin in $H_2{}^{16}O$ at ultrahigh, kHz accuracy. The technique of TPA in a cavity combines high sensitivity with the cancellation of both photon recoil shift and first-order Doppler effect, allowing for an improvement of 4 orders of magnitude in accuracy over previous studies. The present work may be considered as a proof of concept, showing the feasibility of measuring TPA in water at low pressures and relatively large detunings from intermediate states within the two-photon level scheme. Water, as an asymmetric top molecule, exhibits a wealth of TPA resonances to be explored.

## EXPERIMENTAL METHOD

The present TPA study was performed in the same setup used for measuring saturated absorption Lamb dips on water and hydrogen molecules.[17,19] The NICE-OHMS technique, with its characteristic frequency sideband modulations, was employed for sensitive detection.[8,9] A frequency comb laser referenced to a GPS-disciplined oscillator (GPSDO) provided absolute calibration to the kHz level. All measurements were performed at a stabilized temperature of 300 K. The injection and evacuation of the gas from the cavity were continuous and performed through the same connection point. A temperature-controlled capacitive gauge (Pfeiffer CMR 375), zeroed at $10^{-6}$ Pa, was used for pressure measurements. The pressure was stabilized within 2% of its set value using a Proportional/Integral controller running on an Arduino R4 minima that reads the sample pressure through the gauge. The controller regulates the injection of pure water vapor into the cavity via a solenoid valve (Bürkert type 2871).[39,40] This vapor is drawn directly from the headspace of an evacuated glass bulb containing liquid distilled water. This injection system allows for automated pressure studies.

The optical setup utilizes a high-finesse ($\mathcal{F} \approx 150000$) plano-concave cavity (length 371 mm, curved mirror radius 4 m) establishing a beam waist of $w_0 = 0.71$ mm. Because the corresponding Rayleigh range ($z_R \approx 1.16$ m) significantly exceeds the cavity length, the beam expands by only ~ 5% across the active interaction volume. This strong collimation rigorously justifies approximating the beam radius as a constant $w_0$ when evaluating the transit-time limit.

For the wm-NICE-OHMS technique, the spectroscopy laser is phase-modulated inside an electro-optical modulator to generate sidebands at a frequency exactly matching the free spectral range (FSR) of the cavity, $\nu_{FSR} = 404$ MHz. To further reduce noise and enable wavelength-modulation spectroscopy, an additional, lower-frequency dither at 1.2 kHz is applied to the piezo-actuated cavity mirror. The resulting signal is then demodulated and retrieved using a lock-in amplifier. Further details on the NICE-OHMS implementation can be found in an earlier publication.[41]

The observed scatter of individual line centers in Figure 3 significantly exceeds their statistical fitting uncertainties due to the frequency instability of the reference GPSDO (Jackson Laboratories Fury). While a full spectral scan takes 8 min, the central resonance is traversed in just ≈ 100 s. At these integration times, the active disciplining of Oven-Controlled Crystal Oscillators (OCXO) induces short-term frequency excursions with a peak-to-peak wander reaching $1 \times 10^{-10}$.[42] At our ≈ 218 THz probing frequency, this translates to absolute offsets up to ≈ 20 kHz. Because the clock frequency remains relatively stable during the fast line-center crossing, individual fits yield small uncertainties; however, macroscopic wander between successive scans fully accounts for the ≈ 10 kHz scatter observed in Figure 3. Over a large ensemble, this wander acts as a random process, and is intrinsically captured by the standard error of the mean. However, because our 16 scans might not completely average out the clock-induced noise, we adopt a conservative approach. We calculate the final statistical uncertainty of each measurement by adding the standard error of the mean and the residual clock instability in quadrature.

From an experimental perspective, the present study demonstrates that TPA can be achieved for the water molecule at pressures of 0.1 Pa, where pressure broadening is minimal. This is in contrast to the discovery experiment in $N_2O$, where 100 Pa pressures had to be used for obtaining signal.[11] At such high pressure collisional effects cause rather large line broadening. Another key factor is that, presently, TPA was achieved for an intermediate resonance detuned by 127 GHz, whereas for $N_2O$, a detuning as small as 3.5 GHz delivered a signal. In a later $^{13}CO_2$ study, TPA was achieved at 30 Pa and for a detuning of 5 GHz.[15] It may be noted that asymmetric top molecules, with their much denser quantum level structure, will most likely exhibit more intermediate resonances at lesser detunings, ensuring an excellent working ground for TPA.

## ASSOCIATED CONTENT

### Supporting Information

The Supporting Information is available free of charge at https://pubs.acs.org/doi/10.1021/acs.jpclett.6c02007.

Notes detailing the work. S1: Detailed derivation of the transit-time-limited TPA linewidth. S2: Expected line-shape of TPA resonances in the transit-time-limited regime: cusp, wavelength modulation and lock-in detection. (PDF)

Downloaded from pubs.acs.org/jpclcd/article-pdf/doi/10.1021/acs.jpclett.6c02007/6742887/2/acs.jpclett.6c02007.pdf by UNIV CATHOLIQUE DE LOUVAIN user on 27 August 2026



https://doi.org/10.1021/acs.jpclett.6c02007
J. Phys. Chem. Lett. XXXX, XXX, XXX−XXX

## AUTHOR INFORMATION


### Corresponding Author

**Clément Lauzin** − *Institute of Condensed Matter and Nanosciences, Université catholique de Louvain, 1348 Louvain-la-Neuve, Belgium;* orcid.org/0000-0001-5044-5137; Email: clement.lauzin@uclouvain.be

### Authors

**Arthémise Altman** − *Institute of Condensed Matter and Nanosciences, Université catholique de Louvain, BE-1348 Louvain-la-Neuve, Belgium;* orcid.org/0009-0000-3924-3497

**Frank M. J. Cozijn** − *Institute of Condensed Matter and Nanosciences, Université catholique de Louvain, BE-1348 Louvain-la-Neuve, Belgium*

**Alexandr S. Bogomolov** − *Institute of Condensed Matter and Nanosciences, Université catholique de Louvain, BE-1348 Louvain-la-Neuve, Belgium;* orcid.org/0000-0002-6675-0969

**Roland Tóbiás** − *Department of Chemistry, University of Vermont, Burlington, Vermont 05405, United States;* orcid.org/0000-0003-3674-5066

**Attila G. Császár** − *Institute of Chemistry, ELTE Eötvös Loránd University, H-1518 Budapest, Hungary*

**Wim Ubachs** − *Department of Physics and Astronomy, LaserLab, Vrije Universiteit De Boelelaan 1100, 1081 HZ Amsterdam, The Netherlands;* orcid.org/0000-0001-7840-3756

Complete contact information is available at: https://pubs.acs.org/10.1021/acs.jpclett.6c02007


### Notes

The authors declare no competing financial interest.

## ACKNOWLEDGMENTS

The work was supported by the Fonds de la Recherche Scientifique − FNRS (CDR grant no. J.0113.23 and MIS grant no. F.4038.24). FMJ Cozijn is a Chargé de recherche of the Fonds de la Recherche Scientifique − FNRS. ASB is supported by a Marie Curie fellowship provided by the EU Horizon 2023 programme. The work of AGC and RT is supported by the National Research, Development and Innovation Office of Hungary, grant no. 152791 and PD145972. CL thanks the support of the Région Wallonne and LAS&O. With the support of the Walloon Region - SPW-EER - Project PTE VOLET SPATIAL - Grant agreement no. 2110235.

## REFERENCES


(1) Gianfrani, L.; Hu, S.-M.; Ubachs, W. Advances in cavity-enhanced methods for high precision molecular spectroscopy and test of fundamental physics. *Rivista Nuovo Cimento* **2024**, *47*, 229−298.

(2) Wang, J.; Sun, Y. R.; Tao, L.-G.; Liu, A.-W.; Hu, S.-M. Communication: Molecular near-infrared transitions determined with sub-kHz accuracy. *J. Chem. Phys.* **2017**, *147*, 091103.

(3) Reed, Z. D.; Long, D. A.; Fleurbaey, H.; Hodges, J. T. SI-traceable molecular transition frequency measurements at the $10^{-12}$ relative uncertainty level. *Optica* **2020**, *7*, 1209−1220.

(4) Gianfrani, L. Linking the thermodynamic temperature to an optical frequency: recent advances in Doppler broadening thermometry. *Philos. Trans. R. Soc. A* **2016**, *374*, 20150047.

(5) Huang, Q.; Wang, J.; Yin, R.-H.; Tan, Y.; Cheng, C.-F.; Sun, Y. R.; Liu, A.-W.; Hu, S.-M. Cavity-enhanced Doppler-broadening thermometry via all-frequency metrology. *Phys. Rev. Lett.* **2025**, *135*, 223002.

(6) Tao, L.-G.; Liu, A.-W.; Pachucki, K.; Komasa, J.; Sun, Y. R.; Wang, J.; Hu, S.-M. Toward a Determination of the Proton-Electron Mass Ratio from the Lamb-Dip Measurement of HD. *Phys. Rev. Lett.* **2018**, *120*, 153001.

(7) Cozijn, F. M. J.; Dupré, P.; Salumbides, E. J.; Eikema, K. S. E.; Ubachs, W. Sub-Doppler Frequency Metrology in HD for Tests of Fundamental Physics. *Phys. Rev. Lett.* **2018**, *120*, 153002.

(8) Ye, J.; Ma, L.-S.; Hall, J. Sub-Doppler optical frequency reference at 1.064$\mu$m by means of ultrasensitive cavity-enhanced frequency modulation spectroscopy of a $C_2HD$ overtone transition. *Opt. Lett.* **1996**, *21*, 1000−1002.

(9) Foltynowicz, A.; Schmidt, F.; Ma, W.; Axner, O. Noise-immune cavity-enhanced optical heterodyne molecular spectroscopy: Current status and future potential. *Appl. Phys. B: Laser Opt.* **2008**, *92*, 313−326.

(10) Lehmann, K. K. Resonance enhanced two-photon cavity ring-down spectroscopy of vibrational overtone bands: A proposal. *J. Chem. Phys.* **2019**, *151*, 144201.

(11) Zhao, G.; Bailey, D. M.; Fleisher, A. J.; Hodges, J. T.; Lehmann, K. K. Doppler-free two-photon cavity ring-down spectroscopy of a nitrous oxide ($N_2O$) vibrational overtone transition. *Phys. Rev. A* **2020**, *101*, 062509.

(12) Vasilenko, L. S.; Chebotaev, V. P.; Shishaev, A. V. Line shape of two-photon absorption in a standing-wave field in a gas. *JETP Lett.* **1970**, *12*, 161.

(13) Biraben, F.; Cagnac, B.; Grynberg, G. Experimental evidence of two-photon transition without Doppler broadening. *Phys. Rev. Lett.* **1974**, *32*, 643−645.

(14) Abella, I. D. Optical double-photon absorption in Cesium vapor. *Phys. Rev. Lett.* **1962**, *9*, 453−455.

(15) Liu, Y.-Z.; Yu, M.-Y.; Tan, Y.-D.; Wang, J.; Cheng, C.-F.; Jiang, W.; Hu, S.-M. Midinfrared Cavity-Enhanced Two-Photon Absorption Spectroscopy for Selective Detection of Trace Gases. *Anal. Chem.* **2025**, *97*, 848−853.

(16) Tan, Y. D.; Liu, Y. Z.; Yu, M. Y.; Wang, Z. N.; Cheng, C. F.; Hu, S. M. Detecting $^{14}CO_2$ with two-photon absorption spectroscopy. *Sens. Act. B: Chemical* **2026**, *450*, 139265.

(17) Cozijn, F. M. J.; Diouf, M. L.; Ubachs, W. Lamb dip of a quadrupole transition in $H_2$. *Phys. Rev. Lett.* **2023**, *131*, 073001.

(18) Lehmann, K. K. Two-photon absorption line shapes in the transit-time limit. *J. Chem. Phys.* **2021**, *154*, 104105.

(19) Tóbiás, R.; Furtenbacher, T.; Simko, I.; Császár, A. G.; Diouf, M. L.; Cozijn, F. M. J.; Staa, J. M.; Salumbides, E. J.; Ubachs, W. Spectroscopic-network-assisted precision spectroscopy and its application to water. *Nature Comm.* **2020**, *11*, 1709.

(20) Diouf, M. L.; Tóbiás, R.; van der Schaaf, T. S.; Cozijn, F. M. J.; Salumbides, E. J.; Császár, A. G.; Ubachs, W. Ultraprecise relative energies in the (2 0 0) vibrational band of $H_2{}^{16}O$. *Mol. Phys.* **2022**, *120*, e2050430.

(21) Altman, A.; Tóbiás, R.; Bogomolov, A. S.; Diouf, M. L.; Cozijn, F. M. J.; Császár, A. G.; Lauzin, C.; Ubachs, W. Precise frequencies of $H_2{}^{16}O$ lines protected for radio astronomy. *Astroph. J. Suppl. Ser.* **2025**, *280*, 47.

(22) Diouf, M. L.; Tóbiás, R.; Simkó, I.; Cozijn, F. M. J.; Salumbides, E. J.; Ubachs, W.; Császár, A. G. Network-based design of near-infrared Lamb-dip experiments and the determination of pure rotational energies of $H_2{}^{18}O$ at kHz accuracy. *J. Phys. Chem. Ref. Data* **2021**, *50*, 023106.

(23) Cozijn, F. M. J.; Altman, A.; Bogomolov, A. S.; Libert, A.; Collignon, S.; Dierikx, E.; Koelemeij, J. C. J.; Lankhaar, B.; Kleiner, I.; Lauzin, C.; et al. Optically Derived Radio-Frequency Benchmark in Methanol: A Sub-kHz Reference for Astrophysical Tests of Fundamental Physics. *Optica* **2026**, *13*, 1355.

(24) Bordé, C. J.; Hall, J. L.; Kunasz, C. V.; Hummer, D. G. Saturated absorption line shape: Calculation of the transit-time broadening by a perturbation approach. *Phys. Rev. A* **1976**, *14*, 236−263.


Downloaded from pubs.acs.org/jpclcd/article-pdf/doi/10.1021/acs.jpclett.6c02007/6742887/2/acs.jpclett.6c02007.pdf by UNIV CATHOLIQUE DE LOUVAIN user on 27 August 2026

(25) Demtröder, W. *Laser Spectroscopy*, 4th ed.; Springer, 2008.
(26) Dunham, J. L. The energy levels of a rotating vibrator. *Phys. Rev.* **1932**, *41*, 721−731.
(27) Toth, R. A. Extensive measurements of $H_2{}^{16}O$: frequencies and strengths: 5750 to 7965 $cm^{-1}$. *Appl. Opt.* **1994**, *33*, 4851−4867.
(28) Starikov, V.; Mikhailenko, S. Analysis of experimental data for the first hexad (040), (120), (200), (002), (021), (101) of $H_2O$ molecule interacting states. *J. Mol. Struct.* **1998**, *442*, 39−53.
(29) Császár, A. G.; Furtenbacher, T. Spectroscopic networks. *J. Mol. Spectrosc.* **2011**, *266*, 99−103.
(30) Tóbiás, R.; Diouf, M. L.; Cozijn, F. M. J.; Ubachs, W.; Császár, A. G. All paths lead to hubs in the spectroscopic networks of water isotopologues $H_2{}^{16}O$ and $H_2{}^{18}O$. *Commun. Chem.* **2024**, *7*, 34.
(31) Ubachs, W.; Császár, A. G.; Diouf, M. L.; Cozijn, F. M. J.; Tóbiás, R. A network approach for the accurate characterization of water lines observable in astronomical masers and extragalactic environments. *ACS Earth Space Chem.* **2024**, *8*, 1901−1912.
(32) Kukolich, S. G. Measurement of the molecular *g* values in $H_2O$ and $D_2O$ and hyperfine structure in $H_2O$. *J. Chem. Phys.* **1969**, *50*, 3751−3755.
(33) Golubiatnikov, G. Y.; Markov, V. N.; Guarnieri, A.; Knochel, R. Hyperfine structure of $H_2{}^{16}O$ and $H_2{}^{18}O$ measured by Lamb-dip technique in the 180−560 GHz frequency range. *J. Mol. Spectrosc.* **2006**, *240*, 251−254.
(34) Cazzoli, G.; Puzzarini, C.; Harding, M. E.; Gauss, J. The hyperfine structure in the rotational spectrum of water: Lamb-dip technique and quantum-chemical calculations. *Chem. Phys. Lett.* **2009**, *473*, 21−25.
(35) Furtenbacher, T.; Tóbiás, R.; Tennyson, J.; Gamache, R. R.; Császár, A. G. The W2024 database of the water isotopologue $H_2{}^{16}O$. *Sci. Data* **2024**, *11*, 1058.
(36) Schermaul, R.; Learner, R. C. M.; Canas, A. A. D.; Brault, J. W.; Polyansky, O. L.; Belmiloud, D.; Zobov, N. F.; Tennyson, J. Weak line water vapor spectrum in the regions 13 200−15 000 $cm^{-1}$. *J. Mol. Spectrosc.* **2002**, *211*, 169−178.
(37) Tolchenov, R. N.; Naumenko, O.; Zobov, N. F.; Shirin, S. V.; Polyansky, O. L.; Tennyson, J.; Carleer, M.; Coheur, P.-F.; Fally, S.; Jenouvrier, A.; et al. Water vapor line assignments in the 9250−26000 $cm^{-1}$ frequency range. *J. Mol. Spectrosc.* **2005**, *233*, 68−76.
(38) Rogov, M. A.; Zobov, N. F.; Mizus, I. I.; Ovsyannikov, R. I.; Tennyson, J.; Polyansky, O. L. A further step towards a calculated room temperature line list for $H_2{}^{16}O$ with experimental accuracy. *J. Quant. Spectrosc. Rad. Transfer* **2026**, *354*, 109863.
(39) Collignon, S.; Hays, B.; Lederer, D.; Lauzin, C. Precision microwave spectroscopy in a Ku-band waveguide: The case study of the 12.2 GHz line of methanol. *J. Quant. Spectr. Rad. Transfer* **2026**, *353*, 109840.
(40) Kassi, S.; Lauzin, C.; Chaillot, J.; Campargue, A. The (2−0) R(0) and R(1) transition frequencies of HD determined to a $10^{-10}$ relative accuracy by Doppler spectroscopy at 80 K. *Phys. Chem. Chem. Phys.* **2022**, *24*, 23164−23172.
(41) Cozijn, F. M. J. High-precision rovibrational saturation spectroscopy of $H_2$, HD and HT. Ph.D. thesis, Vrije Universiteit, Amsterdam, The Netherlands, 2024.
(42) Pettiti, V.; Cordara, F. Short-term characterization of GPS-disciplined oscillators and field trial for frequency of Italian calibration centers. *Proceedings of the 30th Annual Precise Time and Time Interval (PTTI) Meeting. Reston, Virginia* **1998**, 161−172.

Downloaded from pubs.acs.org/jpclcd/article-pdf/doi/10.1021/acs.jpclett.6c02007/6742887/2/acs.jpclett.6c02007.pdf by UNIV CATHOLIQUE DE LOUVAIN user on 27 August 2026


https://doi.org/10.1021/acs.jpclett.6c02007
*J. Phys. Chem. Lett.* XXXX, XXX, XXX−XXX